NURETH14-39

# EVAPORATION HEAT TRANSFER OF HOT WATER FROM HORIZONTAL FREE SURFACE

Y. Koizumi<sup>1</sup>, Y. Ebihara<sup>1</sup>, T. Hirota<sup>1</sup> and M. Murase<sup>2</sup>

<sup>1</sup>Shinshu University, Ueda, Nagano, Japan

<sup>2</sup>INSS, Mihama-cho, Fukui, Japan

#### **Abstract**

Evaporation heat transfer from the hot water flow to the cold air flow in a horizontal duct was examined. Hot water was in the range of  $35^{\circ}$ C  $\sim 65^{\circ}$ C. Cold air was approximately  $25^{\circ}$ C. The air velocity was varied from 0.0656 m/s  $\sim 1.41$  m/s. The heat transfer rate from the water flow to the air flow became large with an increase in the air velocity. The higher the water temperature was, the larger the heat transfer rate was. When the total heat flux from water to the air flow is divided into two terms; the evaporation term and the forced flow convection term, the evaporation term dominate main part and that is about  $90 \sim 80$  % of the total heat flux. The measured values of the evaporation term and the forced flow convection term were larger than the predicted because of the effect of the diffusion of evaporated vapor. The correlation to predict the heat transfer from the hot water flow to the cold air flow with the evaporation was developed by modifying the laminar flow mass transfer correlation and the laminar forced convection heat transfer correlation. Good results were obtained.

#### 1. Introduction

In Japan, spent fuels of a nuclear reactor are stored in a spent fuel pit in a nuclear power station for a while, and then these are carried to a final disposal and reprocessing plant. When the spent fuels are in the spent fuel pit, decay heat is released from the spent fuels to water in the spent fuel pit. Therefore, the facility of the spent fuel storage has a cooling system. The temperature of water in the spent fuel pit is cooled and maintained below certain temperature by the cooling unit. The spent fuel storage facility has to be inspected regularly. Electricity to the cooling system is turned off during the regular inspection. The power-off results in an increase in the temperature of water in the spent fuel pit. The inspection work has to be finished before the water temperature exceeds

the upper limit that is determined by regulation. Therefore, it is necessary to predict time until the water temperature reaches the upper limit temperature.

Following the concept of the conservatism, the adiabatic condition is assumed at present to predict how long it takes for the water temperature to reach the upper limit. In reality, it may be supposed that heat is transferred from the pool to surroundings. If this heat release is properly taken into consideration to predict the time interval, the time interval would become long. If the time interval becomes long, the inspection work can be performed for sufficient long time. It results in an increase in safety and of course improvement in economy such as a decrease in man power. The present study is intending to provide the realistic method to predict the heat release from the pool to surroundings.

Heat generated in the spent fuels is transferred to water, and then natural convection is formed in the pool water. Thus, the higher the elevation is, the higher the water temperature is in the pool. The surface temperature of the pool water is higher than the temperature of air in the storage building of the spent fuel. Thus, convective heat transfer of air from the surface to air in the building is considered first of all. If the air is not saturated humid air, the evaporation of water may occur at the pool surface. When the evaporation occurs, the evaporated vapor takes the latent heat away from the water since the air temperature is lower than the pool water temperature. It means that the pool water is cooled by the evaporation by itself. Heat is also released from the pool water through the pool wall. However, the thermal conductivity of the concrete of the pool wall and the soil around the pool wall is so small that this heat release may be negligible compared with the former two heat release passes. Therefore, the convective heat transfer of air from the pool surface and the evaporation heat transfer of the hot water are mainly examined in the present study.

There exits forced draft in the storage building of the spent fuels. Therefore, the heat transfer between the hot water surface and the cold air flow were examined in the present study. The combined heat transfer of the convective heat transfer of the air flow and the evaporation heat transfer of water took place simultaneously. It should be noted that the water temperature was higher than that of air and the evaporation of water was not caused by the heat of air.

## 2. Experiment

#### 2.1 Experimental apparatus

An experimental apparatus used in the present study is schematically shown in Figure 1. It was composed of a rectangular test section, a water storage tank, a circulation pump, a compressor and instruments. The test section was placed horizontally. Test fluids were distilled water and air. Water pumped out from the water storage tank flowed through a rotameter into the test section from the bottom inlet at the end of the test section. Water flowed at the bottom part in the test section, flowed out from the bottom outlet at another end of the test section, and returned to the water storage tank. Air supplied from the compressor through a rotameter flowed into the test section from the top inlet at the end of the test section, flowed at the top part of the test section counter-currently to water, and left from the top outlet at the other end of the test section.

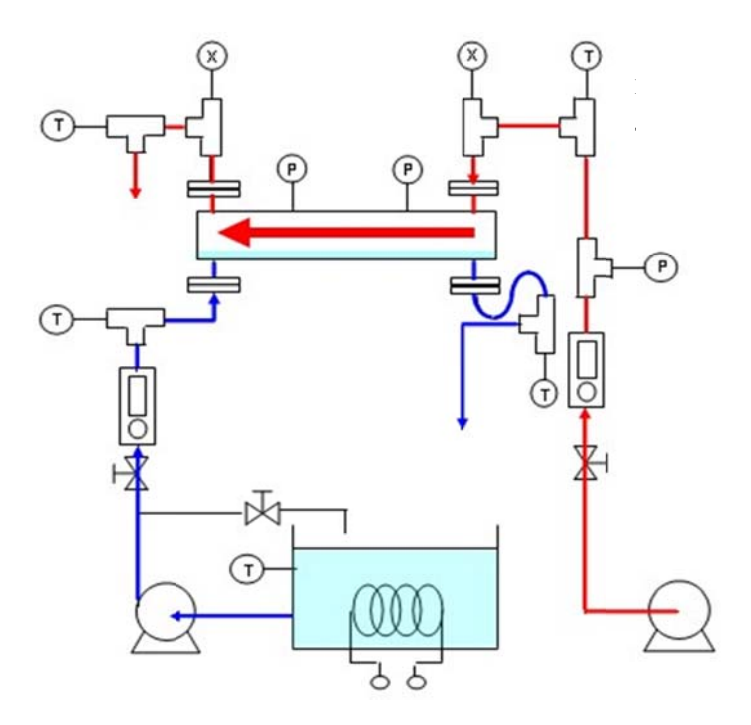


Figure 1 Experimental apparatus

The details of the test section are presented in Figure 2. It was made of transparent Plexiglas. The cross-section of the flow channel was rectangular. The height and the width of the cross-section were 40 mm and 50 mm, respectively. The length of the test section was 600 mm. There were horizontal water splashing preventing plates at the both ends of the test section where there were the inlets and the outlets of water and air.

The level of the plates in the test section was adjustable so as to be the same height as the water level in the test section. The length of the plates was 150 mm. Thus, the actual heat transfer length between water and air was 300 mm. The test section was well thermally insulated with thermal insulator.

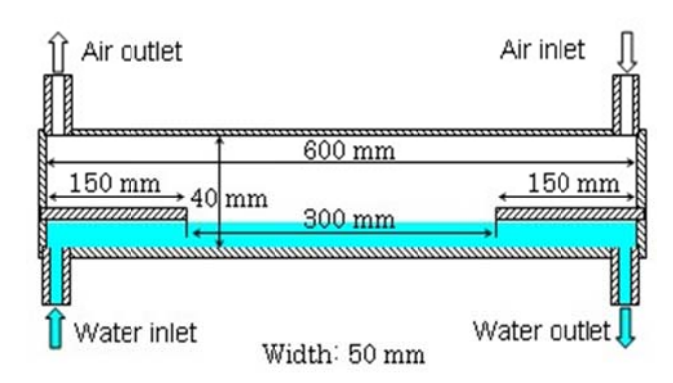


Figure 2 Details of test section

There was an electric heater in the water storage tank. Water temperature was adjusted by the heater.

Water temperature was measured at the inlet and the outlet of the test section with K-type thermo-couples. Temperature, pressure and relative humidity of air were measured at the inlet and the outlet of the test section with K-type thermo-couples, Bourdon tube pressure gauges and electric hygrometers, respectively. The rotameters and the thermo-couples were calibrated prior experiments.

#### 2.2 Experimental procedures

The water depth in the test section was fixed at 5 mm in the present experiments. The average water velocity of the water layer was varied in the range of 0.0253 m/s  $\sim 0.186$  m/s.

Water at the predetermined temperature was supplied to the test section. Then, air was supplied to the test section and fixed at the predetermined flow rate. After it was confirmed that the temperatures of water and air, and the humidity at the inlet and the outlet of the test section were fully stabilized, the temperatures, the pressures, the flow rates and the humidities were measured. Then, the flow rate of air was increased stepwise. This procedure was iterated.

Experiments were performed in the range of  $35^{\circ}\text{C} \sim 65^{\circ}\text{C}$  of water temperature. The air velocity was varied from 0.0656 m/s through 1.41 m/s.

## 3. Experimental results

Air temperatures  $T_{a1}$  and  $T_{a2}$ , and also air pressures  $P_{a1}$  and  $P_{a2}$  were measured at the inlet and the outlet of the air flow, respectively. Relative humidites  $X_1$  and  $X_2$  measured at the inlet and the outlet of the air flow were converted into the inlet and outlet absolute humidities  $x_1$  and  $x_2$  of the air flow by utilizing  $T_{a1}$ ,  $T_{a2}$ ,  $P_{a1}$  and  $P_{a2}$ . Then, inlet and outlet air enthalpies  $h_{a1}$  and  $h_{a2}$  of the air flow were derived by using  $T_{a1}$ ,  $T_{a2}$ ,  $x_1$  and  $x_2$ . The dry air flow rate  $G_{da}$  in the test flow channel was obtained from  $T_{a1}$ ,  $x_{a1}$  and the air flow rate measured at the inlet.

Since the humid air enthalpy is defined for the unit dry air mass, the total heat transfer rate Q from the water flow to the air flow in the test flow channel is calculated as

$$Q = G_{da} \times (h_{a2} - h_{a1}) \quad . \tag{1}$$

The evaporated mass of water in the test flow channel is the product of the dry air flow rate  $G_{da}$  and the absolute humidity increase  $(x_2 - x_1)$  between the inlet and the outlet of the air flow. A water temperature decrease between the inlet and the outlet of the water flow was small, rather negligible as shown later. When water is at the average temperature  $T_w$  of the inlet and the outlet water temperature, the evaporation heat transfer rate  $Q_E$  form the water flow to the air flow is expressed as

$$Q_E = (x_2 - x_1)G_{da}h'' . (2)$$

Here, h" is the saturated dry steam enthalpy at the temperature T<sub>w</sub>.

The total heat transfer rate from water to the air flow is the sum of the evaporation heat transfer rate  $Q_E$  and the convection heat transfer rate  $Q_C$ . Thus,  $Q_C$  is calculated from Q and  $Q_E$  as

$$Q_C = Q - Q_E$$

(3)

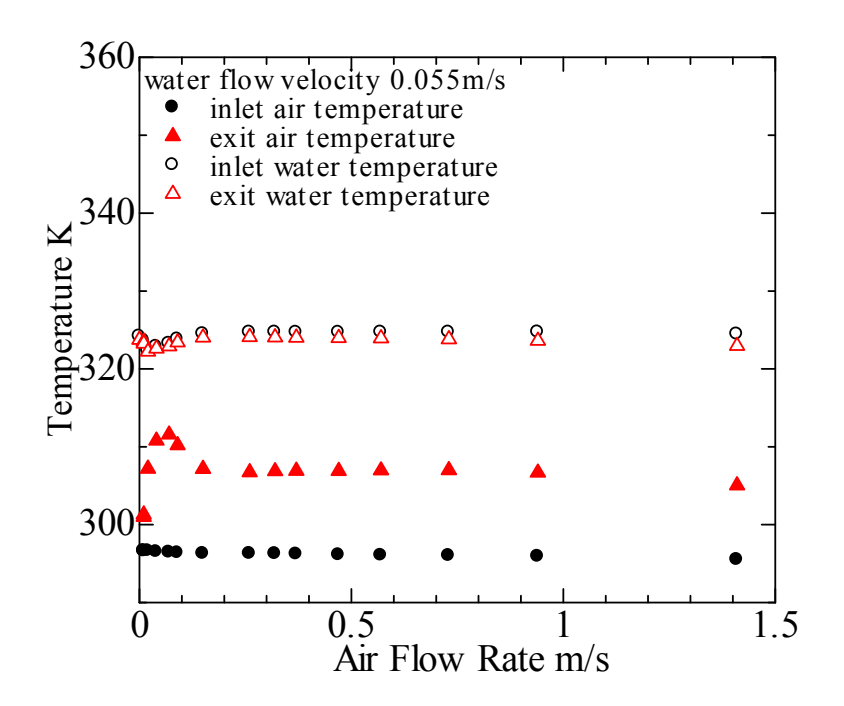


Figure 3 Air and water temperatures

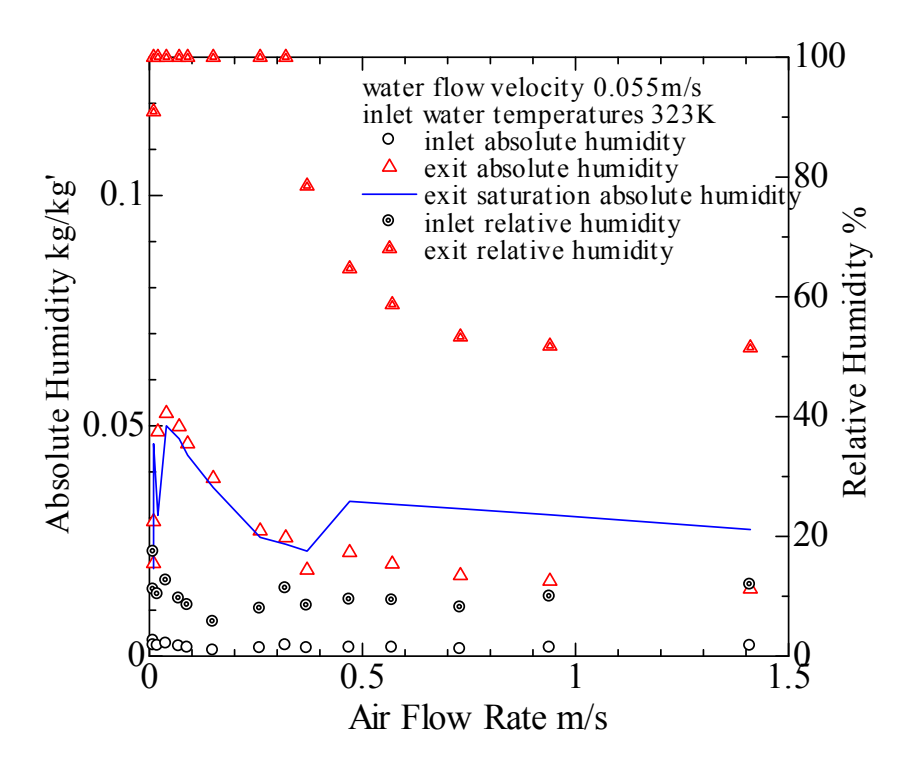


Figure 4 Relative and absolute humidities

Examples of the air and the water temperatures measured at the respective inlet and the outlet are presented in Figure 3. The case shown in the figure is for the water temperature 50 °C and the water velocity  $u_1 = 0.055$  m/s. The relative and the absolute humidities of the air flow at the inlet and the outlet for the same case are also shown in Figure 4. In the figure, the saturated absolute humidity at the outlet of the air flow is also included for comparison. The outlet air temperature is much higher than the inlet air temperature. Although the outlet water temperature is a little bit lower than the inlet water temperature, the difference between the inlet and the outlet is very small. The outlet relative humidity is saturated at the low air flow rate. It decreases as the air flow rate is increased. In the following analyses, the data points that the relative humidity is higher than 95 % are excluded since the accuracy of the electric hygrometer decreases when the relative humidity exceeds 95 %.

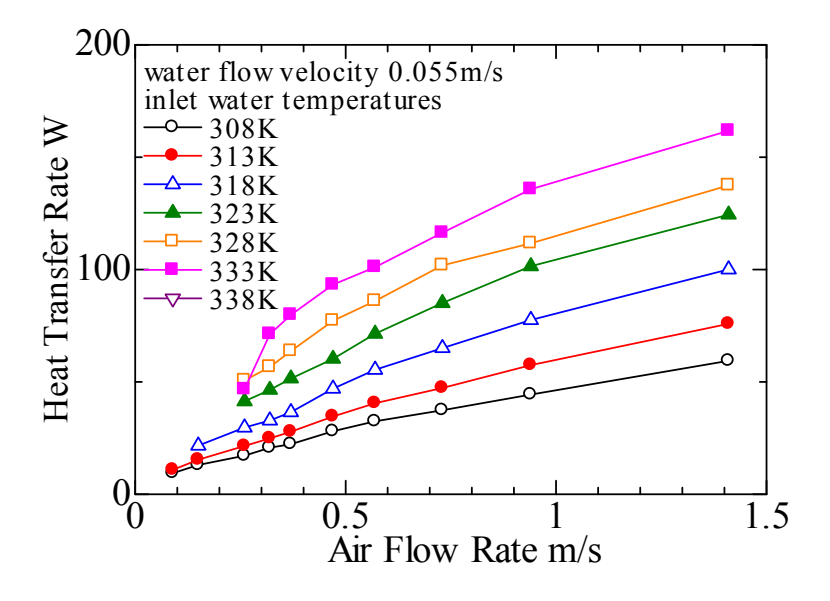


Figure 5 Total heat transfer rate ( $u_1 = 0.055 \text{ m/s}$ )

Total heat transfer rates from water to the air flow are plotted in Figure 5. The case shown in the figure is that the water velocity is 0.055 m/s. The heat transfer rate increases as the water temperature is increased and also the air flow rate is increased.

The ratios of the evaporation heat transfer rate  $Q_E$  to the total heat transfer rate Q are illustrated in Figure 6. Although the ratio decreases a little as the air flow rate is increased, the ratios are approximately 0.8. It implies that the evaporation heat transfer

plays an important role in the heat transfer from hot water to cold air. The water temperature has little effect on the ratio.

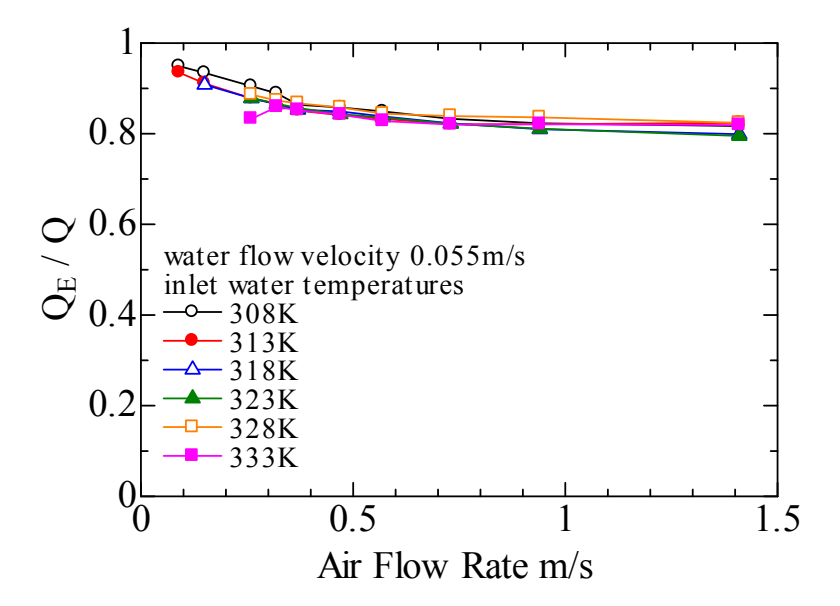


Figure 6 Ratio of evaporation heat transfer rate to total heat transfer rate ( $u_1 = 0.055 \text{ m/s}$ )

#### 4. Analyses

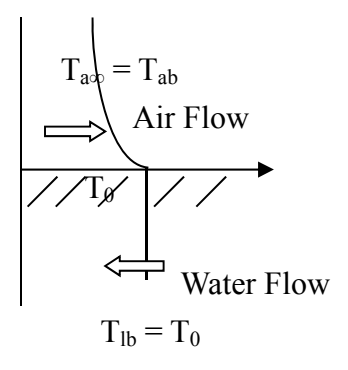


Figure 7 Temperature distribution

The thermal conductivity and the density of water are much larger than those of air. The heat transfer rate from water to air is not so large in the present situation. The difference between the water surface temperature and the water bulk temperature is a few Centigrade at the most for the present condition. Thus, the uniform cross-sectional

temperature distribution is assumed in the water flow as shown in Figure 7. Then, the water surface temperature  $T_0$  equals the water balk temperature  $T_{lb}$ . The air temperature is  $T_0$  at the water surface and  $T_{a\infty}$  at a long distance from the water surface. The temperature  $T_{a\infty}$  is assumed to equal the bulk temperature of the air flow.

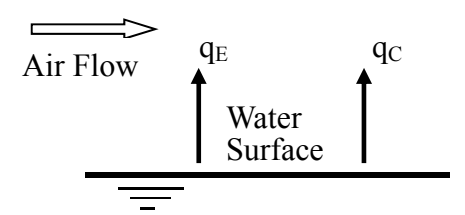


Figure 8 Heat transfer situation

The total heat flux q from the water surface to the air flow is the sum of the evaporation heat flux  $q_E$  and the convection heat flux  $q_C$  as shown in Figure 8;

$$q = q_E + q_C \tag{4}$$

## 4.1 Evaporation heat transfer rate

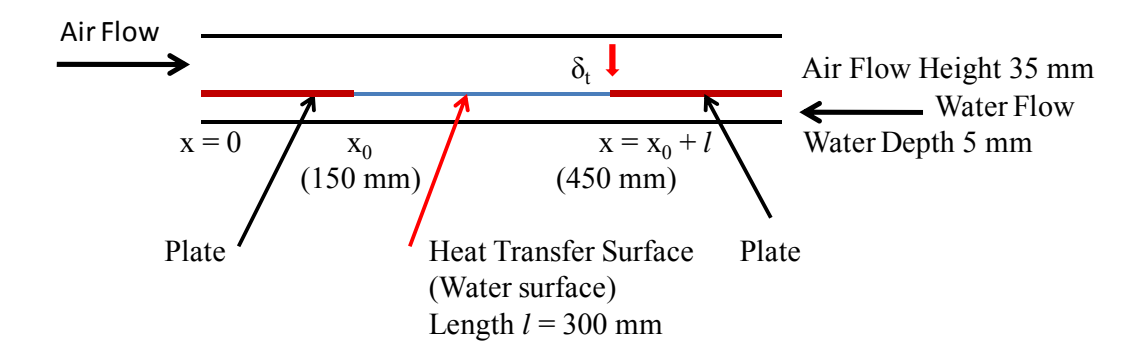


Figure 9 Test flow channel

The test flow channel used in the present experiments is schematically presented in Figure 9. In the test flow channel, there are water splashing preventing plates at the both ends of the test flow channel. It is assumed that het transfer from the water flow to the air flow does not take place at those plates. Thus, the length of the heat transfer surface; the water surface, is 300 mm.

The thickness of the velocity boundary layer of the air flow is given with the following equation<sup>(1)</sup>;

$$\delta = 4.64 \frac{x}{\sqrt{\frac{u_{a\infty}x}{v_{af}}}} \quad . \tag{5}$$

The thickness of the thermal boundary layer of the air flow is also given with the following equation<sup>(1)</sup>;

$$\delta_t = 4.51 \frac{x}{\sqrt{\frac{u_{a\infty}x}{v_{af}}}} \left[ 1 - \left(\frac{x_0}{x}\right)^{3/4} \right]^{1/3} \left(\frac{1}{Pr}\right)^{1/3} . \tag{6}$$

Here, Pr and  $u_{a\infty}$  are the Prandtl number of air and the velocity of the external flow. In the present case,  $u_{a\infty}$  is set to be equal to the air bulk mean velocity in the flow channel. The thickness  $\delta$  and  $\delta_t$  at the end of the heat transfer surface  $x_0 + l = 450$  mm are 11 mm and 9 mm at the most for the present condition. The air space height there is 35 mm. Thus, the flow channel over the heat transfer surface is not filled with the velocity and the thermal boundary layer. It is considered that the flow state is not the flow in the conduit but the flow over the flat plate.

The air in the flow channel in the present case is humid air. Thus, the air is the mixture of dry air and steam. Physical properties should be treated as the mixture of dry air and steam. However, it creates complexity in the calculation. The mass fraction of steam in the humid air is not so large that the physical properties of the humid air is considered to be close to those of dry air. Therefore, the physical properties of dry air are used for the humid air in the following discussions for simplicity.

Since the air Reynolds number  $Re_l = \rho_{da}u_{da}(x_0 + l)/\mu_{da}$  at the end of the heat transfer surface  $x_0 + l = 450$  mm is  $4.2 \times 10^4$  at the most in the present conditions, the boundary layer is laminar. Here,  $u_{da}$  is the velocity of dry air; the air bulk mean velocity in the flow channel. Symbols  $\rho_{da}$  and  $\mu_{da}$  are the density and the viscosity of dry air. Following the analogy from the heat transfer for the laminar flow over the flat plate, the Sherwood number  $S_h$  for the mass transfer for the laminar flow<sup>(2)</sup> is

$$S_h = \frac{h_D l}{D_f} = 0.662 \left( \frac{\rho_{da} u_{da} l}{\mu_{daf}} \right)^{1/2} \left( \frac{v_{daf}}{D_f} \right)^{1/3}. \tag{7}$$

Here, D is the diffusion coefficient of steam in the dry air and  $h_D$  is the mass transfer coefficient of steam by the air flow. The symbol  $v_{da}$  is the dynamic viscosity of dry air. The subscript f denotes the value for the film temperature. Equation (7) is solved for the mass transfer coefficient  $h_D$ . Using it, the evaporation heat flux  $q_E$  is expressed as

$$q_E = \frac{Q_E}{A} = h_D \rho_{da} (w_{v0} - w_{v\infty}) h'' \quad . \tag{8}$$

In this equation, the steam mass fraction in humid air at the water surface;  $w_{v0}$ , is given from the saturated vapor pressure for the water surface temperature. The steam mass fraction  $w_{v\infty}$  at a long distance from the water surface is obtained from the absolute humidity of the bulk flow; the average of the inlet and the outlet absolute humidity. The enthalpy of the dry saturated vapor is denoted h" in the equation. The heat transfer area; the evaporation area, is expressed with A.

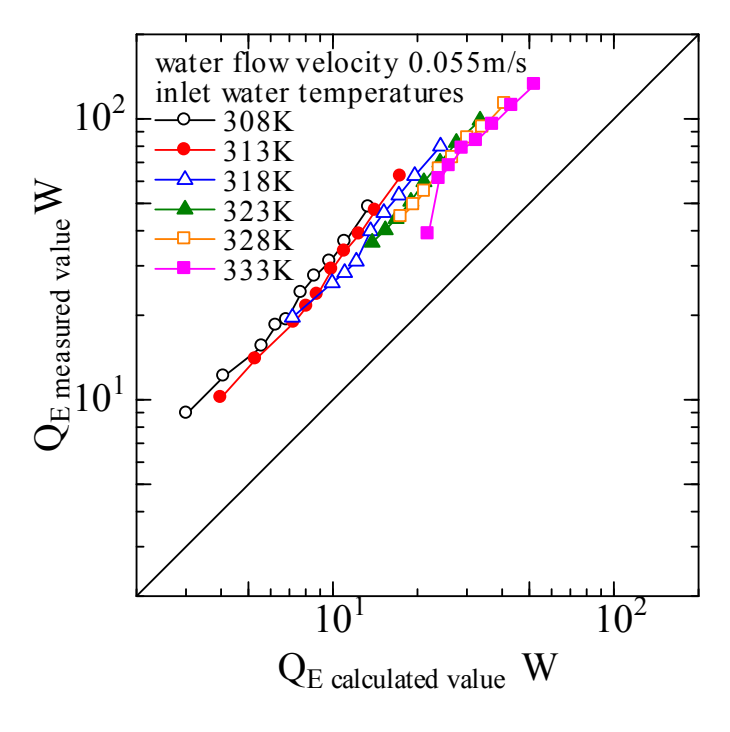


Figure 10 Evaporation heat transfer rate

The heat transfer rates from the water surface to the air flow which are calculated with Equation (8) are compared with the measured results in Figure 10. The case shown in the figure is for the water velocity  $u_l = 0.055$  m/s. The general trend of the measured results is well expressed by the calculation although the measured values are larger than the predicted. Several reasons might be considered why the measured results are larger

than the predicted. The most provable reason is the natural convection effect on the evaporation diffusion since the bottom for the air flow is hotter than the bulk flow of air.

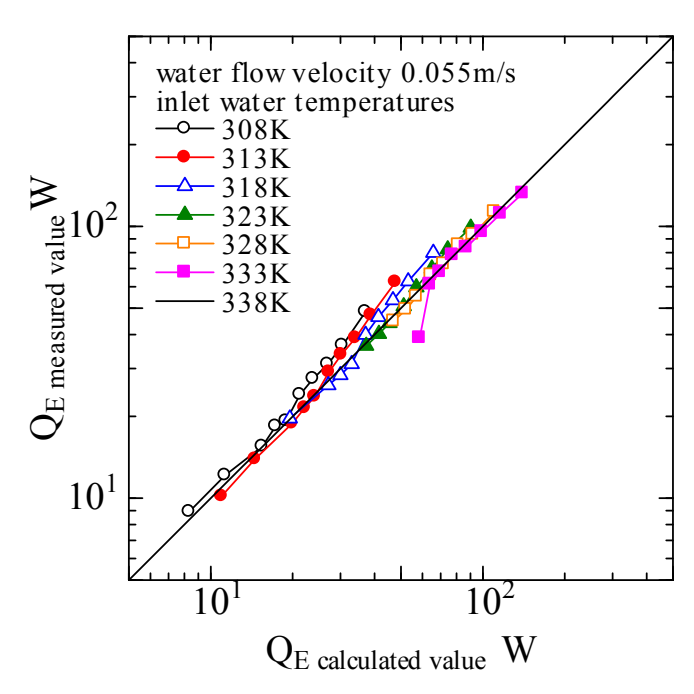


Figure 11 Prediction results of evaporation heat transfer rate with the modified equation  $(u_l = 0.055 \text{ m/s})$ 

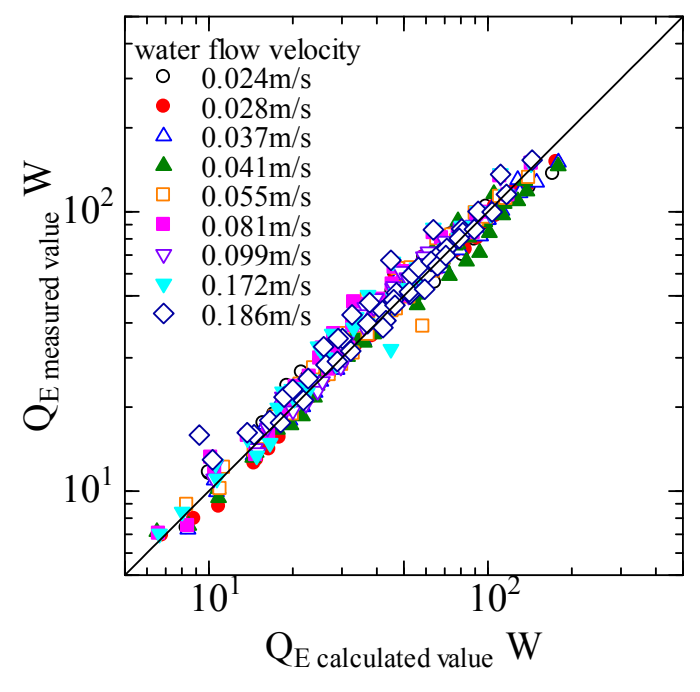


Figure 12 Prediction results of evaporation heat transfer rate with the modified equation (all cases)

By comparing the measured results and the predicted results, Equation (7) is modified to get the best fit with the measured results; the coefficient 0.662 in the right hand of the equation is tuned to 1.93. Prediction results of the evaporation heat transfer rate with the modified equation are presented in Figure 11. The case is again for  $u_l = 0.055$  m/s. Comparison for all conditions in the present experiments is shown in Figure 12. Fine agreement between the prediction and the measured results is obtained in the both figures.

#### 4.2 Convection heat transfer rate

The Nusselt number of the laminar flow heat transfer over the flat plate of the length l is  $^{(1)}$ 

$$Nu = \frac{\alpha_C l}{\lambda_{daf}} = 0.662 \left( \frac{\rho_{da} u_{da} l}{\mu_{daf}} \right)^{1/2} \left( \frac{v_{daf}}{a_{daf}} \right)^{1/3} . \tag{9}$$

The convection heat flux  $q_C$  is calculated with the following equation using the convection heat transfer coefficient  $\alpha_C$  obtained from Equation (9);

$$q_C = \frac{Q_C}{A} = \alpha_C (T_w - T_a) \quad . \tag{10}$$

In Equation (9),  $a_{da}$  and  $\lambda_{da}$  are the thermal diffusivity and the thermal conductivity of dry air, respectively. The average of the inlet and the outlet water temperature is expressed as  $T_w$ , and similarly the average of the inlet and the outlet air temperature is expressed as  $T_a$  in Equation (10).

The ratio of the measured convection heat transfer rate  $Q_E$  to the predicted value with Equation (9) and (10) is defined as

$$\gamma_e = \frac{(Q_E)_{Measurted}}{(Q_E)_{Calculated}} \quad . \tag{11}$$

The values are presented in Figure 13. The value  $\gamma_e$  is greater than 1 and increases with an increase in the air velocity and the water temperature.

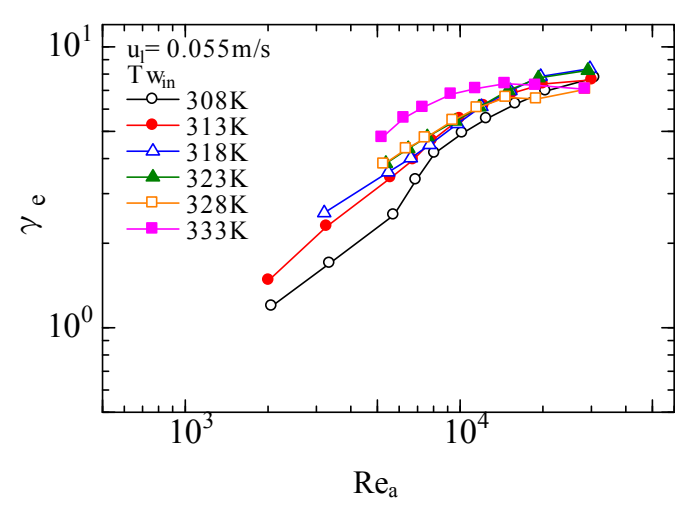


Figure 13 The ratio of the measured convection heat transfer rate to predicted value

Several reasons why the convection heat transfer is enhanced might be considered. The diffusion of the evaporated vapor may have some effect on the temperature gradient. The evaporated vapor may transport sensible heat when it diffuses through air. The diffusion may also create the convection effect on the temperature gradient near water surface. In the present case, the Spolding number B<sup>(3)</sup>

$$B = \frac{c_{pw}(T_{a0} - T_{a\infty})}{H_{fg}} \tag{12}$$

is selected to express these effects. Here,  $c_{pw}$  is the specific heat of steam and  $H_{fg}$  is the latent heat of water at  $T_0$ . To get the best fit of the prediction of the convection heat transfer rate to the measured results,  $\gamma_e$  is correlated with B and the Reynolds  $Re_a = \rho_{da} u_{da} l/\mu_{da}$  number as follows;

$$\gamma_e = (0.076B + 0.05) \text{Re}_a^{1/2}$$
 (13)

The predicted results of the convection heat transfer rate are compared with the measured results in Figures 14 and 15. Figure 14 is for the case of the water velocity  $u_1 = 0.055$  m/s and Figure 15 is for the all cases of the present experiments. In Figure 14, nice agreement is obtained. The predicted results are in good agreement with the measured results in Figure 15 although some deviation is observed at the low heat transfer rate; at the low air velocity, in Figure 15. At the low air flow rate, the exit relative humidity was close to 100 %. The accuracy of the electric hygrometer decreases

when the relative humidity is close to 100 %. The deviation might be caused by it although details are not sure.

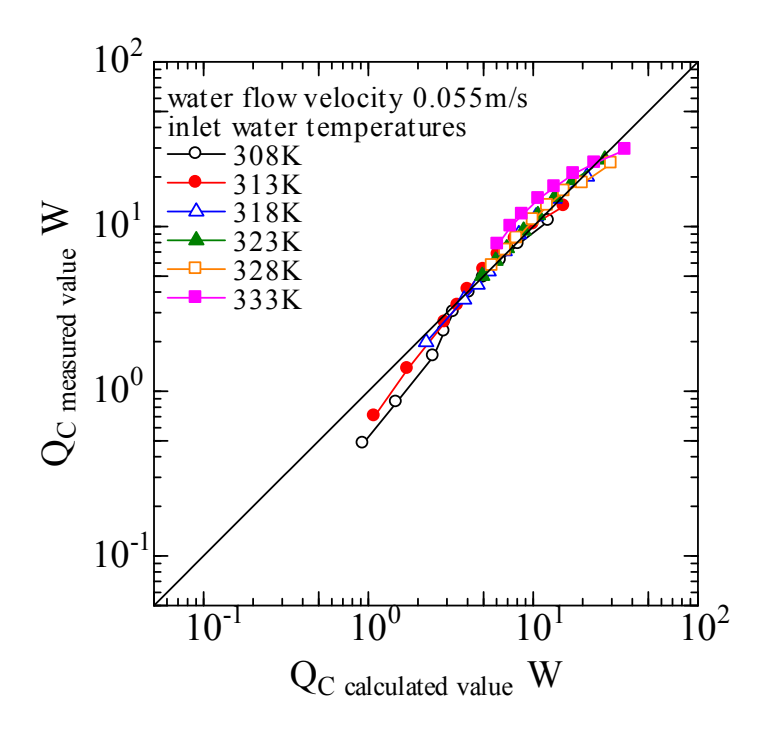


Figure 14 Prediction results of convection heat transfer rate with the modified equation ( $u_1 = 0.055 \text{ m/s}$ )

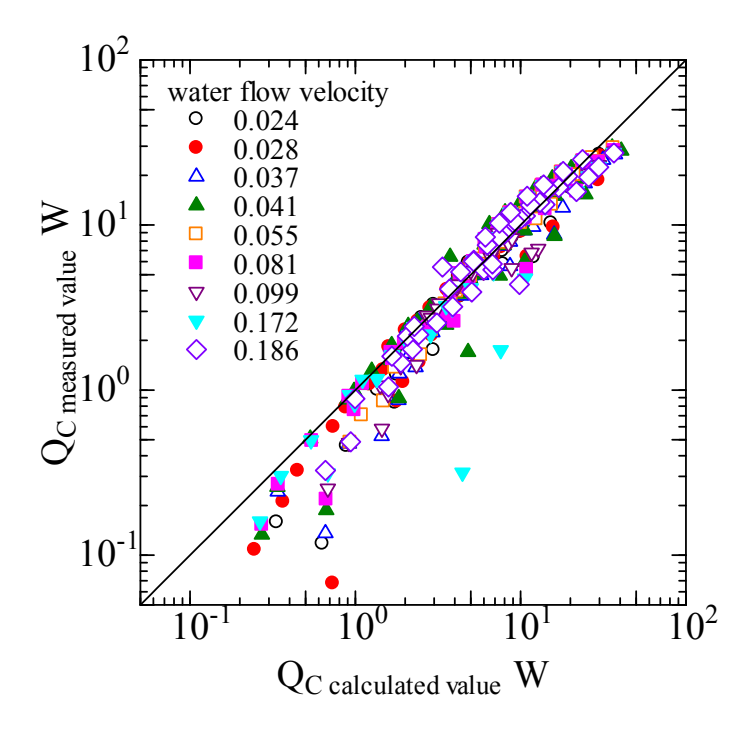


Figure 15 Prediction results of convection heat transfer rate with the modified equation (all cases)

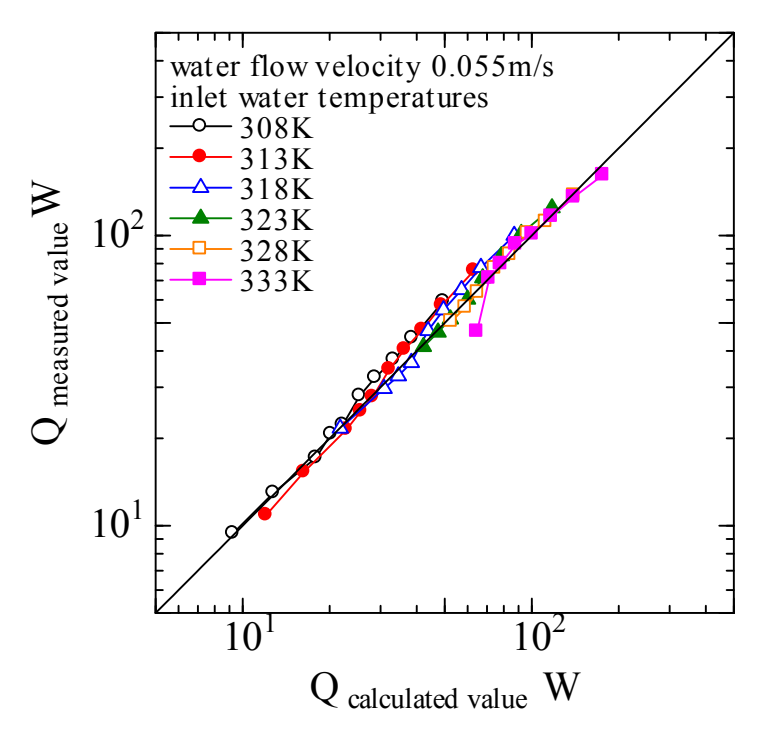


Figure 16 Measured and predicted total heat transfer rate ( $u_1 = 0.055 \text{ m/s}$ )

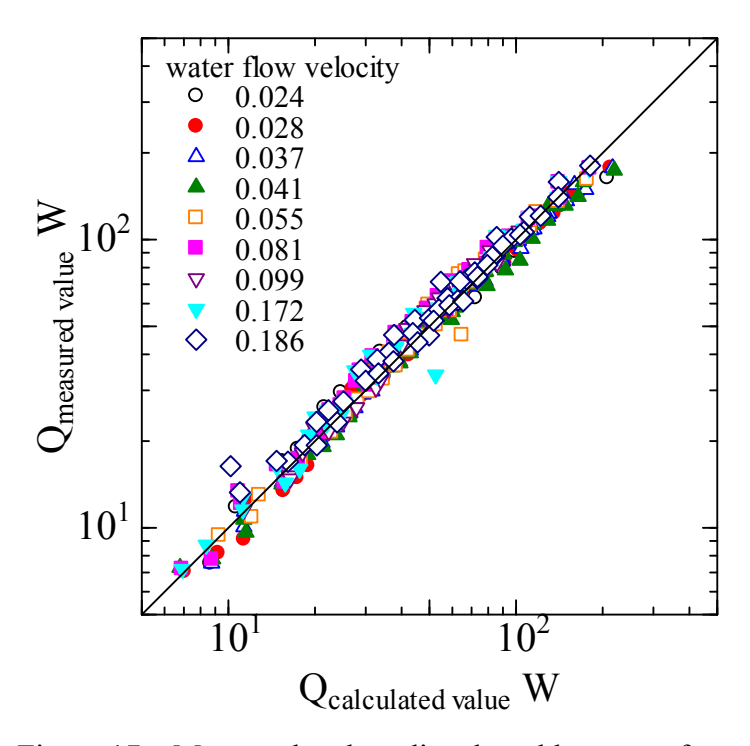


Figure 17 Measured and predicted total heat transfer rate (all cases)

# 4.3 Total heat transfer rate

From above discussions, the total heat transfer rate from hot water to the cold air flow can be calculated with Equations (4), (8), (10) and the followings;

$$Sh = \frac{h_D l}{D} = 1.93 \left(\frac{\rho_{da} u_{da} l}{\mu_{da}}\right)^{1/2} \left(\frac{v_{da}}{D}\right)^{1/3}$$
 and (14)

$$Nu c = \frac{\alpha_c l}{\lambda_a} = 0.662 \left[ (0.076B + 0.05) \text{Re}_a^{1/2} \right] \text{Re}_a^{1/2} \text{Pr}_a^{1/3}$$
(15)

Predicted results with those and the measured results are compared for the case of the water velocity  $u_l = 0.055$  m/s in Figure 16 and for all cases of the present experiments in Figure 17. Good agreement is observed in those figures.

#### 5. Conclusions

Evaporation heat transfer from the hot water flow to the cold air flow in a horizontal duct was examined. Following conclusions were obtained.

- (1) The heat transfer rate from the water flow to the air flow became large with an increase in the air velocity. The higher the water temperature was, the larger the heat transfer rate was.
- (2) When the total heat flux from water to the air flow is divided into two terms; the evaporation term and the forced flow convection term, the evaporation term dominate main part and that is about  $90 \sim 80$  % of the total heat flux.
- (3) The measured values of the evaporation term and the forced flow convection term were larger than the predicted because of the effect of the diffusion of evaporated vapor.
- (4) The correlation to predict the heat transfer from the hot water flow to the cold air flow with the evaporation was developed by modifying the laminar flow mass transfer correlation and the laminar forced convection heat transfer correlation. Good results were obtained.

#### **REFERENCES**

- [1] M. N. Özisik, "Basic Heat Transfer", Robert E. Krieger Publishing Company, Florida, USA, 1987, pp. 210, 218.
- [2] JSME 209. JSME Data Book: Heat Transfer, 5th Edition, Mazruzen Ltd., pp. 85.
- [3] L. L. Ross and T. W. Hoffman, "Evaporation of Droplets in a High Temperature Environment", <u>Proc. of Third Int. Heat Transfer Conference</u>, 1966, pp 50 59.

[4] T. W. Hoffman and L. L. Ross, "A Theoretical Investigation of the Effects of Mass Transfer on Heat Transfer to an Evaporating Droplet", Int. J. Heat Mass Transfer, 15, 1972, pp 599 - 617.